Investigating the optical translucency of Spectralon using BSSRDF measurements

Lou Gevaux, Dipanjana Saha, Gaël Obein

Investigating the optical translucency of Spectralon using BSSRDF measurements

LOU GEVAUX,[1,*] DIPANJANA SAHA,[1] GAËL OBEIN[1]

[1]*LNE-CNAM (EA 2367), La Plaine St Denis, FRANCE*
**Corresponding author: lou.gevaux@lecnam.net*

Author's version, published 15 June 2023, Applied Optics, Vol. 62, Issue 18, pp. 5003-5013, https://doi.org/10.1364/AO.491929

Translucent materials have the property of reflecting light beyond the illumination point due to subsurface light propagation in the material. These reflectance properties can be characterized using the bidirectional scattering-surface reflectance distribution function (BSSRDF), a radiometric quantity which is a function of spatial, angular, spectral and polarisation parameters. At very small scales, we have observed that Spectralon, a commercial material widely used as a diffuse reflectance calibration standard, can be regarded as translucent. This can generate measurement errors and limit Spectralon's reliability as a calibration artefact for instruments that measure optical quantities on very small surfaces. To characterize the translucent properties of Spectralon, we have measured its BSSRDF using an experimental setup based on a goniospectrophotometer with a spatial scanning system for detection. In the present study, we show that Spectralon cannot be considered an opaque material at small scales (below 1 mm). For instrument measuring on small areas, Spectralon can be used for calibration only when the illumination area and the observation area differ by more than 1 mm in radius.

1. INTRODUCTION

Spectralon (Labsphere) is a tradename for sintered polytetrafluoroethylene (PTFE) material [1]. As Spectralon Diffuse Reflectance Standards are durable and stable samples with optical properties close to Lambertian diffusers, they are widely used to calibrate measuring instruments in applications including colorimetry, radiometry, spectroscopy, goniospectrophotometry, remote sensing and imaging. The reliability of Spectralon Standards is crucial to the traceability of the calibrated instruments, so that the measurement results are consistent and can be compared between different instruments and between different laboratories.

Before the commercial production of sintered PTFE by Labsphere in 1986, standards made of packed PTFE were extensively studied by researchers at the National Bureau of Standards (now NIST) [2], and concerns were raised about the translucency of the material, which can lead to a "translucent blurring effect" [3] and induce errors in spectral reflectance measurements (i.e., the "edge loss" phenomenon [4,5]). The translucent blurring effect is described by J. J. Hsia [3] as "the tendency for point irradiation of a sample to produce reflected radiation from a large area of the sample, due to random scattering within the material". In spectrophotometric measurements, it can cause what J. J. Hsia calls "flux loss", whereby, "a portion of the radiation emerges from the surface of a sample beyond the edge of the sample mask (i.e., the receiver collection area) and does not contribute to the response of the receiver, causing measurement errors". As Spectralon is less translucent than packed PTFE and solid PTFE (or Teflon) [6], this issue does not impact measurements in most applications.

However, for measurements on very small areas, Spectralon is sufficiently translucent for the translucent blurring effect phenomenon to be observable and to impact measurements. This is what we observed using our μBRDF measurement facility [7]. With an incident beam of roughly 50 μm diameter, and an observation area of roughly 300 μm, we measured a BRDF value much lower than expected (0.20 sr^{-1} rather than 0.32 sr^{-1} in a 45°:0° geometry at 550 nm), which was the consequence of the edge-loss phenomenon.

A light-scattering material into which light enters and propagates before exiting the material further from its entry point can be described as optically translucent. Following this definition, the classification of a material as translucent or opaque depends on whether the distance travelled by light inside the material can be considered as negligeable or not compared to the typical dimensions of the measurement geometry. For measurement on small areas (submillimetre scale), many materials generally considered as opaque actually show optical translucency, as is the case with Spectralon.

Given the increasing need for measurements on small areas for applications in computer graphics (such as for modelling textiles and hair) or material inspection (measurement of small mechanical parts), we can expect the development of new instruments (colorimeters, spectroradiometers, gonio-spectroradiometers, etc.) designed to measure small areas. These instruments will need to be

calibrated, which means that it is necessary to establish to what scale Spectralon can reliably be used as a calibration standard. This paper proposes to investigate the optical translucency of Spectralon by measuring its bidirectional scattering-surface reflectance distribution function (BSSRDF), towards identifying the scale below which Spectralon's translucency impacts measurement results.

BSSRDF in $m^{-2}.sr^{-1}$ is the quantity that fully describes light interactions with objects made of translucent materials [8,9]. The BSSRDF of a sample is defined as the ratio of reflected radiance $dL_\mathbf{r}$ to incident flux $dF_\mathbf{i}$ when the sample is illuminated on a point by a directional light beam at a wavelength λ and polarization p:

$$BSSRDF(\mathbf{i},\mathbf{r},\mathbf{D},\lambda,p) = \frac{dL_R(\mathbf{i},\mathbf{r},\mathbf{D},\lambda,p)}{dF_I(\mathbf{i},\lambda,p)} \quad (1)$$

As a bidirectional function, BSSRDF depends on the directions of illumination $\mathbf{i}(\theta_\mathbf{i}, \varphi_\mathbf{i})$ and observation $\mathbf{r}(\theta_\mathbf{r}, \varphi_\mathbf{r})$ with (θ, φ) corresponding to the zenith and azimuthal angles respectively. It is also function of the spatial position of the incident beam and of the observation area on the sample. For homogeneous samples, BSSRDF is independent from the incident beam position, and only depends on the vector $\mathbf{D}(x_\mathbf{D}, y_\mathbf{D})$ between the observation area and the point of incidence of the illuminating beam. Consequently, a setup dedicated to BSSRDF measurement must comprise a radiance measurement system capable of observing the surface of the sample at various spatial locations, in addition to a goniometer setup used to control the angular geometry of the measurement. In this work, light is unpolarized and the dependance of BSSRDF on polarization is not studied.

In the definition of BSSRDF, radiance and incident flux are infinitesimal quantities, which means that they are defined for infinitely small surfaces and solid angles, illustrated in Fig. 1. In practice, the incident beam is not perfectly collimated and the incident light flows within a narrow solid angle and hits the surface on a small area. Similarly, the observation area is a small surface, and radiance is measured in a narrow collection solid angle.

The detection system of such a setup can be camera-based, capturing radiance over the entire sample at once [10], or it can rely on a punctual measurement system combined with a spatial scanning system, which measures the sample at several locations by sequentially changing the position of the detector. Each of the two solutions has its advantages and drawbacks and will suit different applications. A camera-based system yields fast measurements with high spatial resolution, which can be a significant advantage for industrial applications. However, calibration is more complex to perform on a camera than on a punctual measurement device like a spectroradiometer, which can pose difficulties regarding traceability for camera-based systems. In addition, BSSRDF measurements require radiance measurements over a high dynamic range (HDR) (more than 6 decades of measurement range), which cannot be achieved with a camera sensor without using an HDR measurement method. Currently, HDR radiance measurements are not traceable to the International System of Units (SI), due to the lack of uncertainty propagation methods when using HDR algorithms. Until this issue is addressed (currently in progress in the Joint Research Program 21NRM01 "HiDyn" [11]), only a punctual measurement system combined with a spatial scanning system can provide traceable measurements and be used to realize the BSSRDF unit. Our laboratory (LNE-CNAM) being the French designated institute for radiometry, photometry and spectrophotometry references, we chose this punctual measurement approach to build a traceable reference measurement setup.

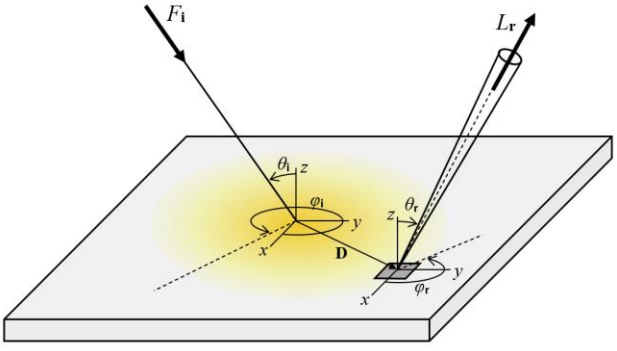

Figure 1. Radiometric quantities and geometrical parameters used to define BSSRDF.

In this article, we describe the design of our BSSRDF measurement setup, detail the BSSRDF measurement equation, and present the measurement values obtained on Spectralon. We then evaluate our measurement results using optical modelling and by comparing them with BRDF results obtained using our primary BRDF goniospectrophotometer, observing that a correction factor is required. Our correction method is verified by making measurements in several configurations. Finally, we propose a simple criterion for determining when Spectralon cannot be used as a reflectance calibration standard as a result of its translucency.

2. MATERIAL AND METHOD

The CNAM goniospectrophotometer setup for BSSRDF measurement, shown in Fig. 2, has been designed to perform an absolute measurement of BSSRDF. It comprises a source, a detector, a sample holder, and shares mechanical parts with our reference goniospectrophotometer and ConDOR facility [12,13]. The sample, held on a robot arm, is illuminated by a directional light beam on a very small area. The reflected radiance is measured over a small area in the direction of observation using a spectroradiometer placed on translation stages to measure radiance at any location on the sample.

To apply the BSSRDF definition given in Eq. (1), the experimental setup must meet a number of requirements:

- The illuminating beam and the observation area must be small, to guarantee a satisfactory spatial resolution. A poor spatial resolution would impact the size of the smallest spatial variations that can be measured, and the high frequency information (located near the illumination point for BSSRDF measurement) would be lost.
- The incident flux must be high and the detection system must be sensitive, to measure the reflected radiance with a satisfactory signal-to-noise ratio. Indeed, outside the illumination area, the fraction of incident light that is collected by the detection system is very small, especially when the sizes of the illumination and observation areas are small.
- The dynamic range of the detection system must be large enough to measure signal inside and outside the illumination area (at least 6 decades of measurement range).

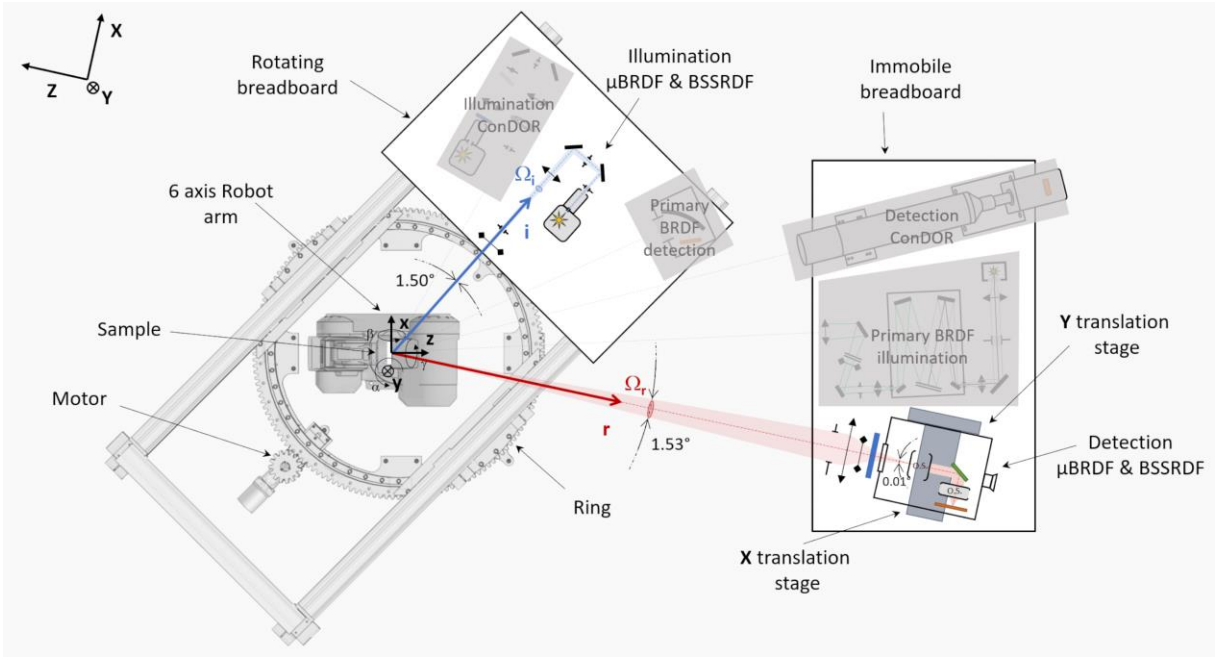

Figure 3. The CNAM goniospectrophotometer setup for BSSRDF measurement (top view). The shaded elements are used for the other types of measurements in the same facility.

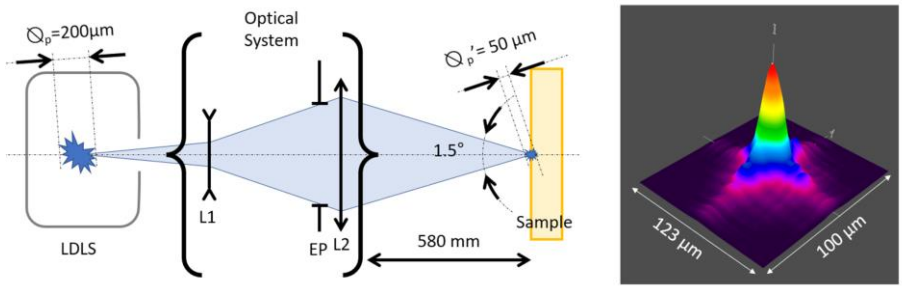

Figure 2. Schema showing the optical design of the source (left) and beam profile on the sample plane measured using a scanning-slit profiling system (right). The beam shape, of diameter $\varnothing_p'$ is the image of the LDLS plasma power repartition, of diameter $\varnothing_p$. The optical system comprises a diverging lens L1, a converging lens L2, and a diaphragm EP that controls the aperture of the beam.

The angular resolution depends on the angular apertures of the source and detection system. For the measurement of a material like Spectralon, this parameter is not especially critical, as the angular variations of its bidirectional reflectance are known to be smooth [14], and we expect similarly smooth variations for BSSRDF.

A. Illumination system

The source of this setup has been designed to illuminate the sample with high irradiance on a very small area. It comprises a laser driver light source (LDLS) (EQ-99X, Hamamatsu) and an optical system optimized to obtain a light dot with a diameter of about 50 µm on the sample (see Fig. 3). The LDLS has been chosen because it emits a high radiance from a small plasma that remains very stable across time. Its power spectral density is similar to a Xenon arc and covers the entire visible spectral range This incoherent, unpolarized and broadband source is shared with CNAM's µBRDF setup and is described in detail in Ref. [7].

The source is located on a breadboard, which is placed over a 360° rotational ring and can be rotated around the sample in the horizontal plane using the rotation ring. The incident flux on the sample is measured by placing the source directly in front of the detection system. The source aperture is adjusted to 1.5°. This angular aperture was chosen as a trade-off between angular resolution and incident flux: a higher angle allows more incident flux, but to the detriment of angular resolution. In addition, the angular aperture of the source cannot be higher than the angular aperture of the detector, otherwise the direct signal cannot be measured without vignetting.

B. Detection system

The detection system is a CS2000 spectroradiometer (Konika Minolta), whose entrance optics have been modified to our needs. The distance between the sample and the spectroradiometer is constrained by our facility and is about 1.7 m. At that distance, the smallest measuring angle of the CS2000 (0.1°) corresponds to an

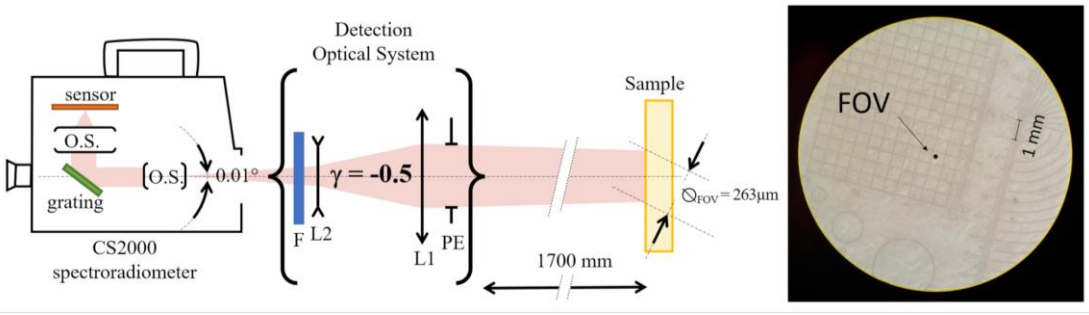

Figure 4. Schema showing the optical design of the detection system (left) and picture taken through the viewfinder of the CS2000 with a micrometric ruler placed on the sample plane, showing the size of the observation area (right).

observation area of about 3 mm on the sample plane, which is too large for BSSRDF measurements. The optics of the CS2000 were consequently removed and replaced by custom optics to obtain an observation area of about 300 µm, which corresponds to roughly 0.01° of angular aperture.

The custom optics were designed to obtain a magnification γ of -0.5 (see Fig. 4). It comprises two achromatic doublets separated by 10 cm, with focal length of 150 mm (L1) and -50 mm (L2). The distance between L2 and the image plane is about 20.5 cm, but as the image plane is difficult to locate precisely inside the CS2000, this distance is adjusted to focus on the sample plane. The diameter of the CS2000 field of view (FOV), evaluated using a micrometric ruler, is $\varnothing_{FOV}$ = 263 µm ± 5 µm.

A filter (F), originally part of the commercial optics, is placed after L2, because spectral calibration of the CS2000 was performed with this filter. The entrance pupil of the system is a diaphragm (PE) placed before L1. This diaphragm controls the aperture of the system and thus, the collection solid angle Ω_r.

The CS2000 is placed on two motorized translation stages and can be translated along the **X** (horizontal) and **Y** (vertical) directions with an uncertainty of 5 µm.

C. Geometry of measurement

The sample is held vertically at the center of the goniospectrophotometer by a 6-axis robot arm (RV-12S, Mitsubishi). Using the robot rotations and the rotation ring, the sample and source are oriented to meet the chosen geometry of measurement for the incident beam and observation direction (**i**, **r**). In theory, all illumination and observation directions of the hemisphere can be reached using this system. In practice, some out-of-plane geometries with high zenithal angles for the observation direction cannot be measured due to collisions between the sample and the robot arm. The angular coverage of the system depends on the size of the measured sample. In addition, a couple of angular geometries are not accessible due to shadows created by other measurement lines of the goniospectrophotometer (ConDOR and Primary BRDF, as illustrated on Fig. 2). For example, BSSRDF cannot be measured at $\mathbf{i}(\theta_i, \varphi_i) = (0°, 0°)$ and $\mathbf{r}(\theta_r, \varphi_r) = (15°, 180°)$ due to the Primary BRDF detection blocking the reflected light. The location of the incident beam on the sample can be controlled by using the translations of the robot arm.

Given the very small incident beam and the small FOV of the detection system, the alignment and angular positioning of the goniometric system must be very accurate. The center of the goniospectrophotometer corresponds to the center of the rotation ring and the center of the robot arm vertical rotation axis. These centers are superposed with an error less than 100 µm. The circularity error of the rotation ring is below 400 µm (the ring is slightly elliptical, 400 µm corresponding to 0.03% of the ring diameter). Two lasers intersecting at the center of the goniospectrophotometer are used to position the sample with an error less than 100 µm. This is sufficiently accurate for classical BRDF measurements, however, for BSSRDF, some positioning errors can be observed in certain geometrical configurations. In such cases, the position of the detector is adjusted manually using micrometric translations. The resulting uncertainties are evaluated by independently repeating the measurement 3 times.

In the sample reference frame, we define the coordinate system (**x**, **y**, **z**) with an origin at the illumination point. To measure the BSSRDF at the location $\mathbf{D}(x_D, y_D, 0)$ in the sample reference frame, the detection system must be translated along the **X** and **Y** axis in the room reference frame of quantities X and Y respectively. For any angular geometry of measurement, the X and Y values can be computed by applying to the vector $\mathbf{D}(x_D, y_D, 0)$ three consecutive rotations of angle β around the **x** axis, α around the **y** axis and γ around the **z** axis, with (α, β, γ) angles describing the orientation of the sample and linked to the angular geometry of measurement $\mathbf{i}(\theta_i, \varphi_i)$ and $\mathbf{r}(\theta_r, \varphi_r)$ using formulas given in Ref. [15]. In the study presented in this paper, only in-plane measurements were performed, which simplifies the calculation of the detector's position:

$$X = x_{\mathbf{D}} \cos\theta_{\mathbf{r}}; Y = y_{\mathbf{D}} \tag{2}$$

D. Measurement model

As expressed in Eq. (1), BSSRDF is a ratio of reflected radiance to incident flux, with the incident flux measured by placing the source directly in front of the detector. In that configuration, the detector measures the radiance L_{source} and the associated dark signal $L_{source,dark}$. The incident flux is calculated using the following equation, with A_{FOV} the area of the detector FOV on the sample plane and Ω_r the observation solid angle:

$$F_{\mathbf{i}} = (L_{source} - L_{source,dark}) A_{FOV} \Omega_{\mathbf{r}} \tag{3}$$

The reflected radiance L_r and its associated dark signal $L_{r,dark}$ are

measured after placing the source, the detection and the sample is the chosen geometry of measurement (**i**, **r**, **D**).

The measurement equation for BSSRDF is:

$$BSSRDF(\mathbf{i},\mathbf{r},\mathbf{D}) = \frac{L_r(\mathbf{i},\mathbf{r},\mathbf{D}) - L_{r,dark}(\mathbf{i},\mathbf{r},\mathbf{D})}{(L_{source} - L_{source,dark})} \frac{1}{A_{FOV}\Omega_r} \quad (4)$$

3. MEASUREMENT RESULTS ON SPECTRALON

The experimental setup described in Section 2 was used to measure BSSRDF on a Spectralon sample of 99% nominal reflectance. The sample was placed on the robot arm and aligned at the center of the goniospectrophotometer. The sample was oriented with its normal direction in the same plane as the incident and observation directions (the horizontal plane of the room) to perform an in-plane measurement. The geometry of measurement was $\mathbf{i}(\theta_i, \varphi_i) = (0°, 0°)$ and $\mathbf{r}(\theta_r, \varphi_r) = (10°, 180°)$. In the following, this in-plane geometry will be noted as (0°:10°). BSSRDF was calculated after measuring the incident flux and reflected radiance as described below.

A. Reflected radiance measurement

The CS2000 was translated in the **X**-**Y** plane, the vertical plane normal to the CS2000 optical axis, to perform measurements around the illumination area. More precisely, with the origin of the coordinates system corresponding to the point of illumination, the CS2000 was translated from -1800 µm to 1800 µm in the **X** and **Y** directions with a step of 300 µm.

Outside the illumination area, the radiance reflected by Spectralon is small, and measuring it with the CS2000 takes roughly 4 minutes per point. To reduce the overall measurement time, points further than 2000 µm from the illumination area were not measured, as no light was expected to be reflected so far from the illumination area.

This long measurement time also impacted the amount of noise in the measured values. To obtain a better signal-to-noise ratio, we decided to compute luminance by multiplying the measured spectral radiance with the V(λ) function [16] and by integrating over the visible spectrum. This comes at a cost to spectral resolution, however, for a first study on Spectralon, this "photometric" BSSRDF already shows results that are of interest, which may be refined in the future with further measurements at selected wavelengths.

The measured values are proportional to a luminance in cd·m^{-2}, but the actual luminance values are unknown due to the loss of the CS2000 spectroradiometer calibration when the entrance optics were modified. However, this is not an issue for BSSRDF calculation, as this unknown calibration coefficient applies to both the incident flux measurement and reflected luminance measurement.

B. Incident flux measurement

The source was rotated directly in front of the CS2000 to measure L_{source} and its associated dark signal. The detector FOV on the sample plane has an area A_{FOV} =5.43E-8 m^2. The observation solid angle Ω_r is 5.61E-4 sr, calculated from the sample to entrance aperture distance (1683.7 mm) and the aperture diameter (45.0 mm). Using these values, the incident flux can be calculated using Eq. (3).

C. BSSRDF results

BSSRDF was computed using Eq. (4) and results for the (0°:10°) configuration are shown in Fig 5. Figure 6 shows the Spectralon illuminated by the microbeam seen through the viewfinder of the CS2000 spectroradiometer.

The standard measurement uncertainty can be evaluated by combining the standard uncertainties associated to each variable of Eq.(4) [17]:

$$\frac{u_{BSSRDF}}{BSSRDF} = \sqrt{\left(\frac{u_{A_{FOV}}}{A_{FOV}}\right)^2 + \left(\frac{u_{\Omega_r}}{\Omega_r}\right)^2 + \left(\frac{u_{L_{source}}}{L_{source}}\right)^2 + \frac{u_{L_r}^2 + u_{L_{r,dark}}^2}{\left(L_r - L_{r,dark}\right)^2}} \quad (5)$$

The uncertainty on the measured signal u_{Lr} is evaluated using the standard deviation of several luminance measurements performed in a row. This uncertainty depends on the measurement position **D**, ranging from 0.3% near the illumination point, to above

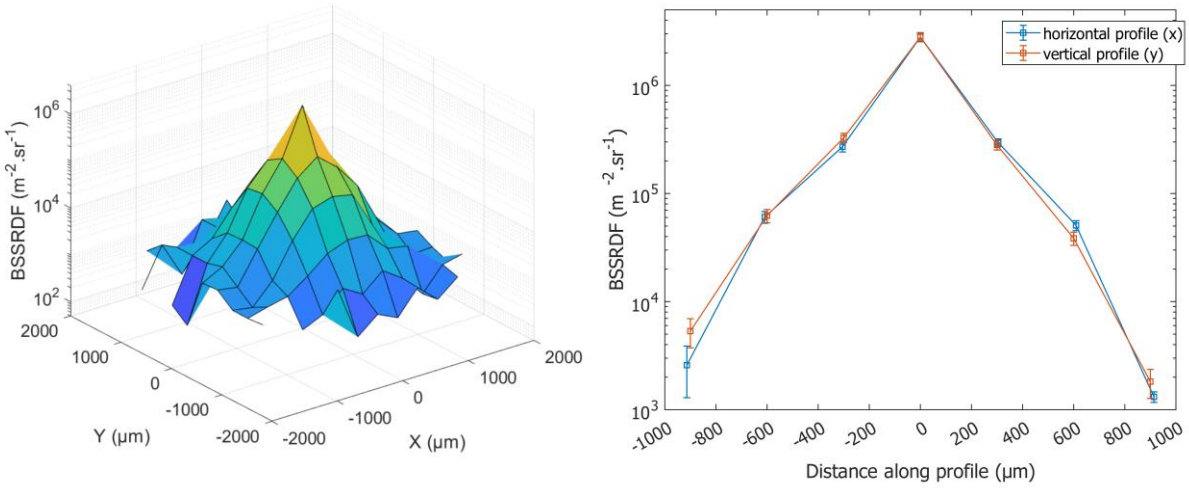

Figure 5. BSSRDF of Spectralon for a (0°:10°) geometry shown in logarithmic scale. Full results (left) and profile along the x axis (blue curve) and the y axis (red curve) (right). The error bars plotted show the expanded uncertainties calculated for 95% confidence (k = 2).

10% far from the illumination point (D>900 μm), where it is the is

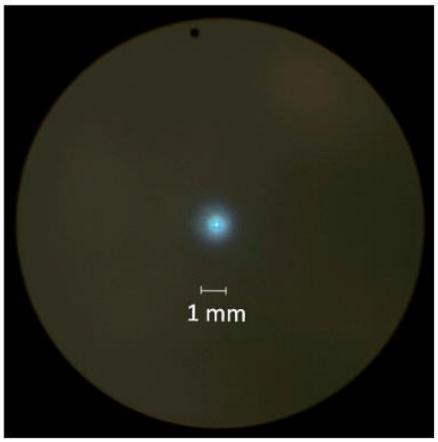

Figure 6. Photo of the sample illuminated by a microbeam observed through the viewfinder of the CS2000 spectroradiometer.

the main source of uncertainty. Near the illumination point, the main source of uncertainty comes from the measurement of the FOV area. The diameter of the FOV has an uncertainty of 5 μm, which results in an uncertainty of 3.8% for the FOV's area.

Table 1. BSSRDF main sources of uncertainty

Uncertainty source	Notation	Value	Comments
Area of the FOV	$\frac{u_{A_{FOV}}}{A_{FOV}}$	3.8%	Calculated from the uncertainty on $\varnothing_{FOV}$
Solid angle	u_{Ω_r} / Ω_r	0.5%	Calculated from the uncertainty on the distance (0.1%) and on the diaphragm diameter (0.2%)
Reading of the source	$\frac{u_{L_{source}}}{L_{source}}$	2%	Evaluated from several readings of the signal, accounts for the source stability and the alignment of the detector by the operator
Reading of the signal - dark	$\frac{u_{L_r}^{\ 2} + u_{L_{r,dark}}^{\ 2}}{\left(L_r - L_{r,dark}\right)^2}$	0.3% - 25%	Evaluated from several readings of the signal
Total	$\frac{u_{BSSRDF}}{BSSRDF}$	4% - 25%	Combined uncertainty expressed for a coverage factor k = 1.

The second highest source of uncertainty comes from the measurement of the source luminance L_{source}, evaluated at 2%. The measured source luminance is strongly impacted by the alignment of the detector. To lower the error on this measurement, the detector is translated by 10 μm steps to find the best position, i.e., the position for which the measured source luminance is maximal.

Finally, the combined uncertainty is below 5% for positions within 600 μm of the illumination point. For future system improvements, we aim to reduce uncertainty to less than 5% for all positions. A simple uncertainty budget presenting the main sources of uncertainty is shown in Table 1.

The BSSRDF measurements have also been repeated 3 times to evaluate their reproducibility. The variations observed on the 3 independent series are lower than the combined uncertainty evaluated in Table 1.

The BSSRDF shown in Fig 5 seems plausible given the pattern of light visually observed on Spectralon through the viewfinder of the CS2000 (see Fig. 6). However, we could not find comparable measurements in the literature to validate this measurement and verify that our results were not impacted by issues such as stray light. Indeed, BSSRDF is computed from a measurement on the sample and a direct measurement on the source, which may both be impacted by a certain amount of stray light. The light reflected by the sample is mostly diffused but the direct light from the source is strongly directional and very bright. Consequently, we do not expect similar levels of stray light for both measurements, which may impact our BSSRDF results.

4. BSSRDF MEASUREMENT EVALUATION

To evaluate our Spectralon BSSRDF measurements, we first evaluated the general shape of the BSSRDF by comparing it with results obtained using optical models. We then evaluated our BSSRDF measurements by comparing them with BRDF measurements, to ascertain whether they were correct in order of magnitude.

A. Evaluation by optical modelling

The interactions between light and translucent materials can be numerically simulated using the diffusion approximation of the radiative transfer theory [18], a model that has the advantage of being simple and that applies well to our study with a directional incident light beam and a dense homogeneous translucent material with very low absorption properties.

The resolution of our observation system (observation over an area of diameter 263 μm) is not small enough for a comparison between the shapes of the measured and modelled BSSRDF for a material like Spectralon, for which the BSSRDF is very steep near the point of illumination. For this reason, we propose to use the spatial repartition of the reflected light around the point of illumination to evaluate the shape of the BSSRDF.

Figure 7 (left) shows the Point Spread Function (PSF) simulated using the diffusion approximation for a directional illumination and a diffuse observation, which depends on the absorption coefficient μ_a, the reduced scattering coefficient μ_s' and the optical index n of the material, as detailed in [5]. This PSF has approximately the same shape as the BSSRDF.

To model the measured BSSRDF, the PSF is convoluted by a disk of the same diameter as the source and then summed over the measurement area, as illustrated in Figure 7 (right). The obtained values simulate the measurement relative to an unknown multiplicative factor. To account for the effects of this unknown multiplicative factor, it is the ratio k of the BSSRDF at the centre of the sample over the sum of the BSSRDF at all the measured positions $\mathbf{D}(x_r, y_r)$ that is compared between the simulation and the experimental measurement:

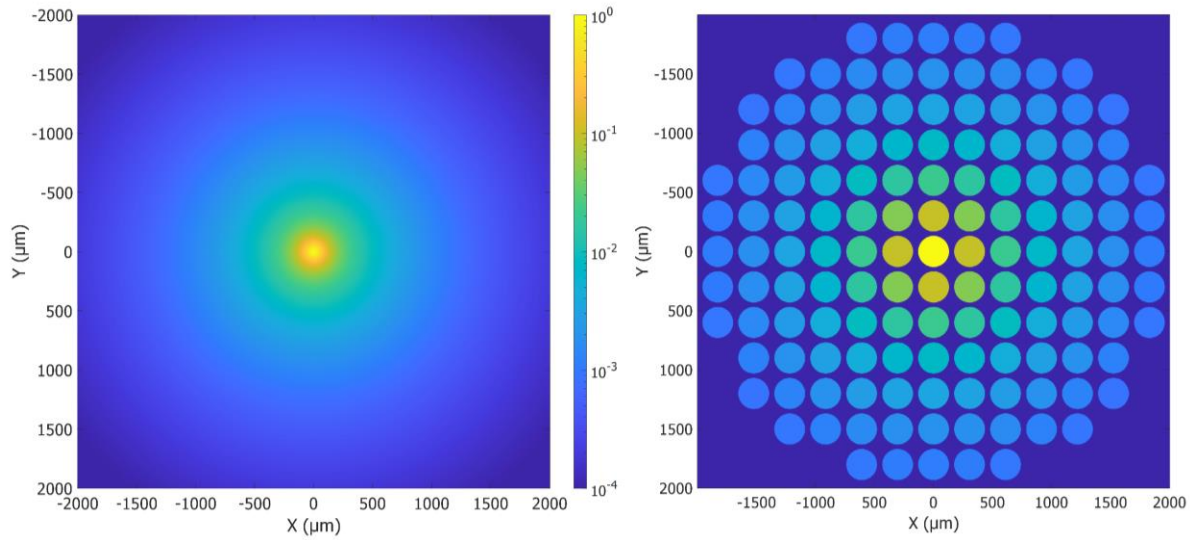

Figure 7. Left: Simulated PSF for a material of optical properties (μa = 0 mm-1; μs'=15 mm-1 and n = 1.4) shown is logarithmic scale and normalized to 1 at the center. Right: Simulated PSF convoluted by the source and averaged over the collection areas corresponding to each of the BSSRDF measurement presented in Figure 5.

$$k = \frac{BSSRDF(0,0)}{\sum_{x_r, y_r} BSSRDF(x_r, y_r)} \tag{6}$$

For the experimental measurements, we obtain $k = 0.55$. For the theoretical simulation, we assume that Spectralon is not absorbing ($\mu_a = 0$ mm^{-1}) and adjust the reduced scattering coefficient μ_s' to best fit the experimental value. The closest k value is obtained for $\mu_s' = 17$ mm^{-1}. The reduced scattering coefficient for Spectralon has been measured by Jensen et al. [18] in the red, green and blue wavelengths : $\mu_{s'\_red} = 11.6$ mm^{-1}; $\mu_{s'\_green} = 20.4$ mm^{-1} ; $\mu_{s'\_blue} = 14.9$ mm^{-1}. Given that our BSSRDF measurement is performed over a V(λ) function, $\mu_s' \sim 17$ mm^{-1} seems compatible with the values found in the literature.

B. Evaluation by comparison with BRDF values

The relation between BSSRDF (in m^{-2}.sr^{-1}) and BRDF (in sr^{-1}) is an integration over an area A around the point of illumination, with A large enough to include all the reflected light [8]:

$$BRDF(\mathbf{i},\mathbf{r}) = \int_{\mathbf{D}\in A} BSSRDF(\mathbf{i},\mathbf{r},\mathbf{D})\,dA \tag{7}$$

This relation can be used to evaluate the validity of our BSSRDF measurements. In this study, we performed a discrete measurement of BSSRDF at locations $\mathbf{D}(x_r, y_r)$ with 300 μm steps (=Δx) in the **X** and **Y** directions. The integral in Eq. (7) consequently becomes a sum over all the measured points, with $dA = \Delta x^2/\cos\theta_r$. Using Eq. (4) as well, Eq. (7) becomes:

$$BRDF(\mathbf{i},\mathbf{r}) = \frac{\sum_{\mathbf{D}(x_r,y_r)} L_r(\mathbf{i},\mathbf{r},\mathbf{D}) - L_{r,dark}(\mathbf{i},\mathbf{r},\mathbf{D})}{(L_{source} - L_{source,dark})} \frac{\Delta x^2}{A_{FOV}\Omega_r \cos\theta_r} \tag{8}$$

Applying Eq. (8) with our measurement values, we obtain a BRDF of 0.455 sr^{-1} for Spectralon at (0°:10°). Measuring the BRDF of the same sample in the same geometry using our Primary BRDF setup, we found a value of 0.331 sr^{-1}.

Several hypotheses for the significant difference between the two measurement values were considered. This error could be caused by a misalignment of the detector for the direct measurement of the source, but multiple independent measurements of the source radiance showed that the uncertainty of this measurement is below 2%, which is much smaller than the error observed. The error could be caused by the non-linearity of the detector, as the luminance measured on the source is 10^6 times larger than the luminance measured on the sample. However, when the source radiance was measured using a calibrated neutral density filter of optical density 3 to evaluate the impact of linearity, no significant variation was observed.

We therefore interpret the error as a consequence of stray light. Stray light is primarily a result of diffraction, diffusion by the optics and mechanical elements, and multiple reflection on lens surfaces. For the direct source measurement, having a non negligeable portion of the incident flux escaping the detection area results in calculating BSSRDF and BRDF values higher than the actual value, which is what we observe here. The measurement error between 0.455 sr^{-1} and 0.331 sr^{-1} would correspond to 27% of the light being lost due to stray light during the direct source measurement.

To verify whether this high amount of stray light was possible or not, we performed a scan of the source: the source was placed opposite the spectroradiometer and measurements were performed after translating the spectroradiometer in the **X** and **Y** directions with steps of 300 μm. A neutral density filter with optical density 4 was used to attenuate the signal and stay within the linearity range of the CS2000 sensor. If there were no stray light, the measurement would show signal when the spectroradiometer is centred on the source, and no signal at any other position, as the source is smaller than the FOV of the spectroradiometer. As shown in Fig. 8, this is not the case. The signal measured at the centre

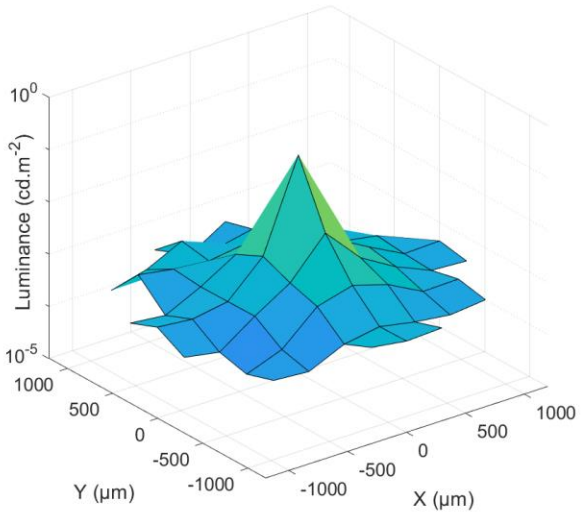

Figure 8. Direct scan of the source in logarithmic scale, showing that light is not only measured when the spectroradiometer is centered on the source, due to stray light in the optics of the spectroradiometer.

corresponds to only 75% of the total measured signal, which gives roughly 25% of the light being lost due to stray light. This is compatible with the error observed on the BRDF estimation.

This source scan gives us an indication of the amount of stray light, but it cannot be used to estimate a correction factor, because translating the spectroradiometer slightly alters the light path in the optical system, which consequently alters the stray light. However, it shows that our CS2000-based detection system is strongly affected by stray light issues and support the hypothesis that this is our main source of error. A possible solution could be to reduce the aperture of the detector to reduce stray light, but this would require us to also reduce the aperture of the source, which would reduce the incident flux and therefore impact the signal-to-noise ratio of the measurements. As such, this option was discarded, and instead, a method to determine a correction factor was sought.

C. Determination of a correction factor

A direct quantification of the amount of stray light is difficult in our case because we don't have access to the image plane of the CS2000 spectroradiometer. Consequently, we need an alternative solution to compute a correction factor.

In the field of BRDF measurement, it is not always possible to perform absolute measurements of the BRDF: the mechanical design of certain goniospectrophotometers does not allow for the measurement of the incident irradiance. In such cases, a calibrated reflectance standard is used to compute BRDF values from relative measurements. The exact same approach cannot be used for BSSRDF, as no certified standard yet exists for this quantity, but a similar approach can be considered. Since we can measure the absolute BRDF of samples using our reference goniospectrophotometer, we propose to use BRDF measurements and the relation between BSSRDF and BRDF given in Eq. (8) to determine a correction factor k_{SL}:

$$k_{SL} = \frac{BRDF(\mathbf{i},\mathbf{r})(L_{source} - L_{source,dark})}{\sum_{\mathbf{D}(x_\mathbf{r},y_\mathbf{r})} L_r(\mathbf{i},\mathbf{r},\mathbf{D}) - L_{r,dark}(\mathbf{i},\mathbf{r},\mathbf{D})} \frac{A_{FOV}\Omega_\mathbf{r}\cos\theta_\mathbf{r}}{\Delta x^2} \quad (9)$$

This allows us to obtain an absolute measurement of BSSRDF, which can also be expressed independently from the source luminance L_{source} and the FOV's area A_{FOV}:

$$BSSRDF(\mathbf{i},\mathbf{r},\mathbf{D}) = \frac{L_r(\mathbf{i},\mathbf{r},\mathbf{D}) - L_{r,dark}(\mathbf{i},\mathbf{r},\mathbf{D})}{\sum_{\mathbf{D}(x_\mathbf{r},y_\mathbf{r})} L_r(\mathbf{i},\mathbf{r},\mathbf{D}) - L_{r,dark}(\mathbf{i},\mathbf{r},\mathbf{D})} \frac{BRDF(\mathbf{i},\mathbf{r})\cos\theta_\mathbf{r}}{\Delta x^2} \quad (10)$$

Although additional sources of uncertainty must be accounted for with this alternative expression of the BSSRDF, this method could allow us to reduce our measurement uncertainties, as two of the main uncertainty sources presented in Table 1 are no longer part of the equation. The correction factor was calculated from two series of measurements, from which the mean value is k_{SL} = 0.73. This value is comparable with the stray light observed on the source direct scan detailed in 4.3.

D. Evaluation of the correction factor

The correction factor calculated from the BRDF and BSSRDF measurements on Spectralon for the (0°:10°) geometry is quite large. Our hypothesis is that this is due to issues with the source direct measurement. To support this hypothesis, measurements at another geometry and on another sample were performed. If the need for a correction factor originates from issues in the source direct measurement, the correction factor should remain the same whatever the sample or the geometry of measurement. This is what we aim to verify in this section.

The measurement protocol described in Section 3 was repeated on the same Spectralon sample for the geometry $\mathbf{i}(\theta_i, \varphi_i)$ = (0°, 0°) and $\mathbf{r}(\theta_r, \varphi_r)$ = (30°, 180°), noted (0°:30°). The BRDF of the sample was measured for this geometry using our Primary BRDF setup. Its value is 0.322 sr^{-1}.

In addition, a highly diffusing sample made of 85% of polyurethane resin and 15 % of titanium dioxide (TiO2) powder was measured using our BSSRDF and BRDF setups at (0°:10°). This "White Resin" sample is less translucent than Spectralon and light does not travel far from the incident point. Consequently, its BSSRDF was measured on a smaller area, at positions ranging from -600 µm to 600 µm in the **X** and **Y** directions with a step of 300 µm. The BRDF value of this sample at the same geometry is 0.296 sr^{-1}.

The correction factors calculated from the different measurements are shown in Table 2. The average value for the correction factor is 0.71. The relative standard deviation observed on the 5 values is 4.1%, which gives an uncertainty on the correction factor of 1.9% assuming a normal distribution. This value is coherent with the uncertainty estimated in Section 3, because it has the same order of magnitude. The good accordance between the correction factors calculated for several measurement configurations and samples confirms that the need for a correction is mainly due to issues with the source direct measurement, namely stray light.

The BSSRDF values measured on Spectralon and White Resin have been corrected using the average correction factor k_{SL} = 0.71.

Profiles of the BSSRDF along the **x** and **y** axis are plotted on Fig. 9 (Spectralon) and Fig. 10 (White Resin).

Table 2. Correction factor estimations on several measurements

Sample, geometry	BRDF obtained from Eq (8)	BRDF	Correction factor
Spectralon, (0°:10°) #1	0.465 sr^{-1}	0.331 sr^{-1}	0.712
Spectralon, (0°:10°) #2	0.445 sr^{-1}	0.331 sr^{-1}	0.744
Spectralon, (0°:30°) #1	0.483 sr^{-1}	0.322 sr^{-1}	0.667
Spectralon, (0°:30°) #2	0.440 sr^{-1}	0.322 sr^{-1}	0.732
White Resin, (0°:10°)	0.413 sr^{-1}	0.296 sr^{-1}	0.717
Average value			0.714

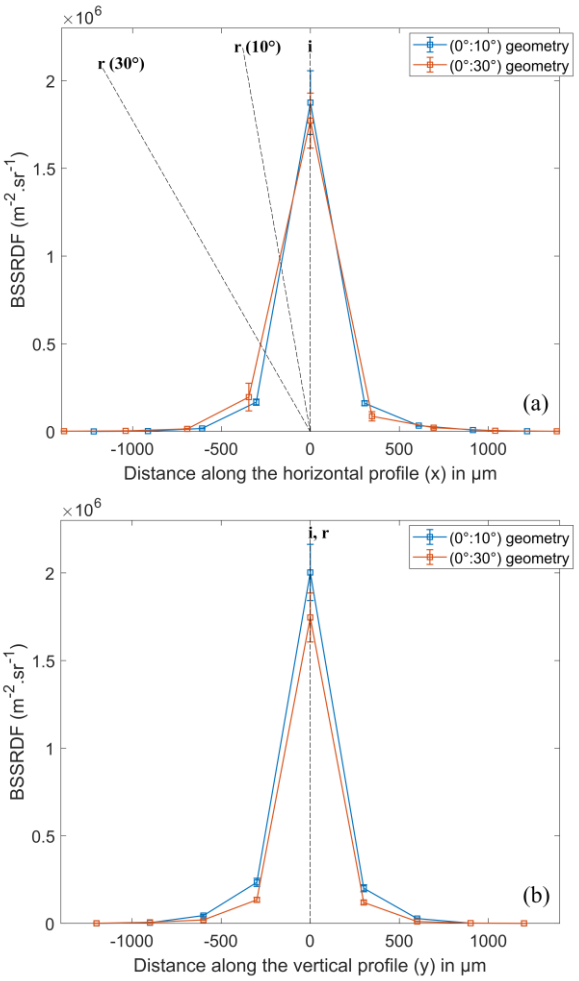

Figure 9. Corrected BSSRDF of Spectralon for (0°:10°) (blue curve) and (0°:30°) (red curve) geometries, in linear scale. Profile along the horizontal direction (**x** axis) (a) and the vertical direction (**y** axis) (b). The error bars plotted show the expanded uncertainties calculated for 95% confidence (k = 2). The dotted lines give the directions of the incident light (**i**) and observation directions (**r**).

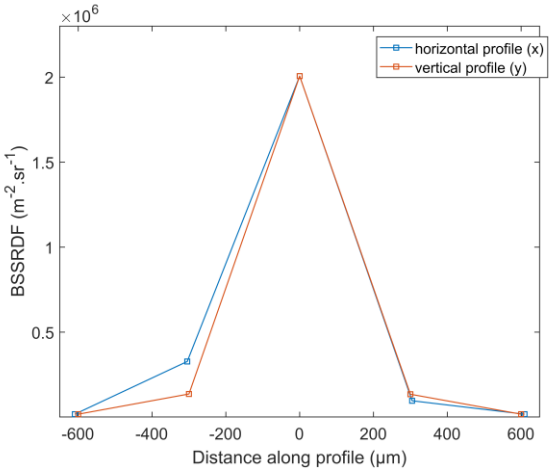

Figure 10. Corrected BSSRDF of the White Resin sample at (0°:10°). Profile along the **x** axis (blue curve) and the **y** axis (red curve).

We can observe on the curves showing Spectralon BSSRDF results on Fig. 9 that the profile along the **x** axis presents a small dissymmetry at (0°:30°) (Fig. 9, left), while this is not observed on the profile along the **y** axis (Fig. 9, right). We can speculate that not only the total amount of diffuse light (i.e., the BRDF) varies with angle, but also that the angular distribution of the diffuse light varies spatially. A more comprehensive study of the variations of Spectralon BSSRDF with angles could be of interest, as it could be compared to data simulated using Monte Carlo models or compared with existing databases of Spectralon angular reflection properties [14].

5. DISCUSSION ON THE TRANSLUCENCY OF SPECTRALON

When looking at a several millimetre thick Spectralon sample, one would generally not judge it to be a translucent material, as one might plastic, marble, or skin. However, at small scales, the impact of translucency on the measured reflectance is not negligeable.

The spatial repartition of the reflected light can be calculated from the BSSRDF measurements results. For Spectralon, roughly 55% of the reflected light is reflected outside the area of observation of our detection system, i.e., within a radius of 132 µm around the illumination point. Consequently, Spectralon cannot be considered an opaque material at small scales, below 1 mm.

The measurement results also indicate that more than 99.9% of the reflected light is reflected within a radius of 1 mm around the illumination point. This allows us to estimate a criterion that must be met to accurately measure the reflectance or BRDF of Spectralon: the difference between the radius of the illumination area and the observation area, illustrated in Fig. 11, should be greater than 1 mm.

6. CONCLUSIONS AND PERSPECTIVES

In this study, we have used an experimental setup to measure the BSSRDF of Spectralon in order to investigate its translucency properties. Two methods have been applied to evaluate the general validity of our measurements. A comparison with an optical simulation relying on the diffusion equation of the radiative transfer shows that our results have the right shape, but a comparison with

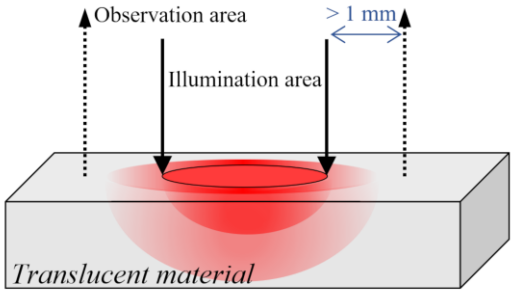

Figure 11. Criterion on the dimensions of the illumination and observation areas required to measure the reflectance properties of Spectralon without error, illustration in the case of an under-filled configuration [5].

BRDF shows that the BSSRDF order of magnitude is erroneous, mainly due to stray light. As a full characterization of stray light to derive a correction factor is difficult, we instead measured the BRDF of the same sample and used the relationship between BRDF and BSSRDF to estimate a correction factor. In this way, we obtained an absolute measurement of BSSRDF. We hypothesized that the correction factor estimated from the BSSRDF and BRDF measurements allows us to correct stray light issues in the source direct measurement. To validate this hypothesis, we performed several measurements on Spectralon at another angular geometry and on another sample, and computed the correction factor associated to each measurement. The standard deviation observed on a series of 5 measurements is compatible with the uncertainty estimated on our BSSRDF measurements, which indicates that our correction method is valid. From the measurement results, we estimate that Spectralon Diffuse Reflectance Standards can be used for calibration when the difference between the radius of the illumination area and of the observation area is superior to 1 mm.The work presented in this article has allowed us to better understand the challenges of BSSRDF measurements. Indeed, BSSRDF is a quantity that depends on 8 parameters, and measuring it requires dealing with multiple constraints to achieve high resolution and good signal-to-noise ratio: 1) the illumination area must be small, not larger than $\mu_s'^{-1}$; 2) the source must be powerful enough to get signal; 3) the detection system must be sensitive enough, to measure luminance lower than 1E-2 cd·m^{-2}; 4) the detection system must observe the sample on a small area, no larger than a few hundred microns; 5) and finally, the detection system must be corrected for stray light. The characteristics of the measuring system will impact the type of material that can be measured. If the signal-to-noise ratio is not sufficiently high, materials of medium to high translucency will not be measurable because the signal will be lost in the noise. If the resolution of the system is not sufficiently high, materials of low to very low translucency will not be measurable because the shape of the BSSRDF will vary over dimensions much smaller than the resolution. It is therefore not an easy task to design a setup able to measure the BSSRDF of samples for a wide range of translucency.

In addition, issues related to stray light strongly impact the measurements. In our case, we used a detection system with only two lenses, and the impact is significant, as shown by the large correction factor. A more ideal setup may be to use a mirror-based optics for the detection system, and it might be necessary to find an alternative to measure the incident flux on the sample. This leads us to speculate that stray light will likely be an issue for camera-based systems, which comprise imaging lenses that are more or less prone to stray light depending on their optical design complexity. This is a useful piece of information in a field where many camera-based instruments are being developed for research and industrial applications.

Today, no certified standard exists for BSSRDF. In the absence of such a standard, the proposed correction method sketches out a possibility for how instruments measuring relative BSSRDF, including camera-based instruments, could be calibrated. Indeed, a method using the mathematical relationship between BSSRDF and BRDF, as well as BRDF absolute measurements, may provide a route to absolute and traceable results.

Although measuring BSSRDF is challenging, it is a task of increasing significance for characterizing the appearance of the objects that surround us. BSSRDF is indeed the only quantity containing all the information required to describe the reflectance properties of objects made of translucent materials, and as shown in this study, below a certain scale, most dielectric materials are translucent. This is especially true for natural and organic materials (plants, fruit and vegetables, biological tissue, etc), but also for manufactured materials such as plastic. The stakes of this field of research are high with applications in fields including medicine, agriculture, computer graphics, manufacturing and 3D printing. We are therefore working toward developing a reference measurement setup that can be used to realise the BSSRDF scale and to characterize samples of varying translucency that can be used as reference standards to help bring the BSSRDF unit to other labs and industry. For this purpose, Spectralon might be considered as a reference sample representing materials of very low translucency.

Funding. This work has been carried out in the frame of the project 18SIB03 BxDiff, that has received funding from the EMPIR program co-financed by the Participating States and from the European Union's Horizon 2020 research and innovation program and in the frame of the ITN that is funded by the European Union's Horizon 2020 research and innovation program under the Marie Skłodowska-Curie grant agreement No. 814158.

Disclosures. The authors declare no conflict of interest.

Data availability. Data underlying the results presented in this paper are not publicly available at this time but may be obtained from the authors upon reasonable request.

References

1. A. Springsteen, "Standards for the measurement of diffuse reflectance - an overview of available materials and measurement laboratories," Analytica Chimica Acta 12 (1999).
2. V. R. Weidner and J. J. Hsia, "Reflection properties of pressed polytetrafluoroethylene powder," J. Opt. Soc. Am. **71**, 856 (1981).
3. J. J. Hsia, "Optical radiation measurements: The translucent blurring effect: method of evaluation and estimation," National Bureau of Standards 38 (1976).
4. J. T. Atkins and F. W. Billemeye, "Edge-loss errors in reflectance and transmittance measurement of translucent materials," Materials Research and Standards **6**, 564 (1966).
5. L. Gevaux, L. Simonot, R. Clerc, M. Gerardin, and M. Hebert, "Evaluating edge loss in the reflectance measurement of translucent materials," Appl. Opt. **59**, 8939 (2020).
6. B. K. Tsai, D. W. Allen, L. M. Hanssen, B. Wilthan, and J. Zeng, "A comparison of optical properties between solid PTFE (Teflon) and (low

density) sintered PTFE," in Z.-H. Gu and L. M. Hanssen, eds. (2008), p. 70650Y.
7. D. Saha, L. Gevaux, T. Cances, A. Richard, and G. Obein, "Development of a µBRDF goniospectrophotometer for BRDF measurement on tiny surfaces," in *Proceedings of the Conference CIE 2021* (International Commission on Illumination, CIE, 2021), pp. 327–334.
8. F. E. Nicodemus, J. C. Richmond, J. J. Hsia, I. W. Ginsberg, and T. Limperis, *Geometrical Considerations and Nomenclature for Reflectance*, 0 ed. (National Bureau of Standards, 1977), p. NBS MONO 160.
9. A. Ferrero, J. R. Frisvad, L. Simonot, P. Santafé, A. Schirmacher, J. Campos, and M. Hebert, "Fundamental scattering quantities for the determination of reflectance and transmittance," Opt. Express **29**, 219 (2021).
10. P. Santafé-Gabarda, A. Ferrero, N. Tejedor-Sierra, and J. Campos, "Primary facility for traceable measurement of the BSSRDF," Opt. Express **29**, 34175 (2021).
11. JRP 21NRM01 "HiDyn" of the Euramet Metrology Partnership program, "https://www.hidyn.ptb.de".
12. G. Obein, S. Ouarets, and G. Ged, "Evaluation of the shape of the specular peak for high glossy surfaces," in M. V. Ortiz Segovia, P. Urban, and J. P. Allebach, eds. (2014), p. 901805.
13. R. Le Breton, G. Ged, and G. Obein, "Out of plane BRDF Measurement at LNE-Cnam using "ConDOR", our primary goniospectrophotometer," in *Proceedings of the 28th Session of the CIE* (2015), pp. 1401–1407.
14. C. Bruegge, N. Chrien, and D. Haner, "A Spectralon BRF data base for MISR calibration applications," Remote Sensing of Environment **77**, 354–366 (2001).
15. G. Obein, R. Bousquet, and M. E. Nadal, "New NIST Reference Goniospectrometer," in Proceedings of SPIE - Optical Diagnostics (2005), Vol. 5880, pp. 241–250.
16. *Standard CIE 018:2019*, (CIE, CIE Central Bureau, Vienna, 2019).
17. BIPM, IEC, IFCC, ILAC, ISO, IUPAC, IUPAP, and OIM, "Evaluation of measurement data. Guide to the expression of uncertainty in measurement. Joint Committee for Guides in Metrology, JCGM," (2008).
18. H. W. Jensen, S. R. Marschner, M. Levoy, and P. Hanrahan, "A practical model for subsurface light transport," in *Proceedings of the 28th Annual Conference on Computer Graphics and Interactive Techniques - SIGGRAPH '01* (ACM Press, 2001), pp. 511–518.